Different and Identical Features of Chondroblastic Osteosarcoma and Chondrosarcoma: Highlights on Radiography and Magnetic Resonance Imaging

Chao-Hsuan Yen[1,3,4], Cheng-Yen Chang[1,3]*, Michael Mu-Huo Teng[1,3,4], Hung-Ta H. Wu[1,3], Paul Chih-Hsueh Chen[2,3], Hong-Jen Chiou[1,3], Nai-Chi Chiu[1,3]

Departments of [1]Radiology and [2]Pathology, Taipei Veterans General Hospital, and [3]Faculty of Medicine and [4]Department of Biomedical Imaging and Radiological Sciences, National Yang-Ming University School of Medicine, Taipei, Taiwan, R.O.C.

Background: To identify the different and identical features of 2 tumors with similar pathologic findings, chondroblastic osteosarcoma (OGS) and chondrosarcoma (CSA), with highlights on radiography and magnetic resonance imaging (MRI).
Methods: Ten patients with chondroblastic OGS and 10 patients with CSA were enrolled. After recording the tumor location, tumor morphology was evaluated for patterns of bony destruction, visible tumor matrix, and aggressive periosteal reactions, endosteal scalloping, cortical expansion, cortical breakthrough and pathologic fracture by radiographic analysis. Signal intensity changes, enhancement pattern, and tumor extensions were evaluated by MRI.
Results: The mean patient ages were 24.7 and 56.7 years in patients with chondroblastic OGS and CSA, respectively ($p = 0.001$). Tumor occurrence was detected in the appendicular bones in 8 chondroblastic OGS and 3 CSA. Three chondroblastic OGS occurred around the knee ($p = 0.003$). In addition, there were 6 tumors arising from the metaphysis and 2 arising from the diaphysis in chondroblastic OGS patients. In CSA patients, 1 tumor arose in the metaphysis, 1 in the diaphysis, and 1 in the epiphysis ($p = 0.039$). On radiographs, visible bone-forming tumor matrix was present in 8 chondroblastic OGS, and coexistence of bone- and cartilage-forming patterns were detected in 2. Visible cartilage-forming tumor matrix was present in 7 CSA, and atypical radiodensity patterns were detected in 2 ($p < 0.001$). Aggressive periosteal reaction was present in 7 chondroblastic OGS, and non-aggressive periosteal reaction was found in 1 CSA ($p = 0.008$). MRI revealed the presence of a lobular structure of high signal intensity on T2-weighted images, and peripheral rim and septal enhancement pattern was noted in 2 chondroblastic OGS and 10 CSA patients. Inhomogeneous and marginal enhancement patterns were noted in 6 and 2 chondroblastic OGS, respectively ($p = 0.001$).
Conclusion: Metaphysis origin, bone-forming tumor matrix, aggressive periosteal reaction, and young patient age favored chondroblastic OGS. Some chondroblastic OGS showed radiologic and MRI appearances that were typical of CSA. [*J Chin Med Assoc* 2009;72(2):76–82]

Key Words: bone neoplasms, chondrosarcoma, magnetic resonance imaging, osteosarcoma, radiography

Introduction

The World Health Organization (WHO) subdivides conventional osteosarcoma (OGS) into osteoblastic, fibroblastic, and chondroblastic subtypes, depending on the predominance of the tumor matrix,[1–3] while the tumor matrix of chondrosarcoma (CSA) is uniformly and entirely chondroid in nature. Thus, tumors that exhibit neoplastic bone-forming capabilities in addition to cartilaginous differentiation should not be classified as CSA, but are a chondroblastic subtype of OGS.[1]

Clinical outcome of OGS has dramatically improved over the past decades,[3,4] mostly due to response to preoperative chemotherapy. Surgery is the standard treatment of CSA.[5–7] Thus, correct pathologic preoperative diagnosis is very important for management decisions. Only when the essential tumor aspect of neoplastic bone differentiation is biopsied can pathologists make the

*Correspondence to: Dr Cheng-Yen Chang, Department of Radiology, Taipei Veterans General Hospital, 201, Section 2, Shih-Pai Road, Taipei 112, Taiwan, R.O.C.
E-mail: cmychang@vghtpe.gov.tw • Received: November 10, 2008 • Accepted: February 10, 2009

correct diagnosis of chondroblastic OGS. Otherwise, a misdiagnosis of CSA might occur. Therefore, radiologists play a crucial role in biopsy planning. Under the guidance of preoperative imaging, the accuracy of an image-guided biopsy might be greatly improved.

Although the imaging features of conventional OGS and CSA are well known, few studies have focused on the imaging characteristics of chondroblastic OGS.[3,8–10] Therefore, identification of the different and common imaging features of chondroblastic OGS and CSA, reflecting pathohistologically different sarcomatous cells and common hyaline cartilage components, was undertaken in this study. Avoidance of the common features during biopsy planning in patients with OGS will improve biopsy accuracy and lead to differential treatment strategies.

Methods

A retrospective review of the pathological database in Taipei Veterans General Hospital was conducted from February 2002 to January 2008, and included 14 patients with chondroblastic OGS and 29 with CSA. After exclusion of 7 patients with extraskeletal CSA, 4 with chondroblastic OGS, and 12 CSA cases without available preoperative radiographs or magnetic resonance imaging (MRI), 10 chondroblastic OGS and 10 CSA (7 grade 2 tumors, 3 grade 3 tumors) patients were included in this study. All images were evaluated and met consensus by Dr Chang and Dr Yen, who have 10 and 2 years experience in the analysis of musculoskeletal images, respectively.

Nine patients with chondroblastic OGS received a combination of preoperative chemotherapy and surgery, and 1 patient received chemotherapy only. All 10 CSA patients received surgery. All 10 patients with chondroblastic OGS and 7 patients with CSA were followed-up (mean duration of 1.9 years) regularly in the outpatient department of Taipei Veterans General Hospital. For patients with regular follow-up, local tumor recurrence occurred in 1 chondroblastic OGS and 3 CSA patients, distant metastasis occurred in 5 chondroblastic OGS and 1 CSA patients, and death from the tumors occurred in 2 chondroblastic OGS patients.

Tumor location in the skeleton (appendicular or axial bones) and tumor distribution in a single bone (in transverse and longitudinal planes) were documented. In the transverse plane, lesions occurred in central (close to the central axis of the bone) or peripheral (in 1 side of the central axis of the bone, still within the medullary canal) locations. In the longitudinal plane, lesions in tubular bone developed in the epiphysis, metaphysis, and diaphysis.

Tumor morphology was evaluated for the pattern of bone destruction and visible tumor matrix, and the presence of aggressive or non-aggressive periosteal reaction, endosteal scalloping, cortical expansion, cortical penetration, and pathologic fracture by radiograph analysis.

MRI analysis was performed using a GE Signa Excite 1.5T and HD 1.5T (GE Healthcare, Milwaukee, WI, USA). Pre-intravenous gadolinium T1- and fat-saturated T2-weighted images as well as post-intravenous gadolinium T1- and fat-saturated T2-weighted images on axial, coronal, or sagittal planes were analyzed. Furthermore, signal intensity changes, enhancement pattern, and full extension of the tumor were evaluated. To determine the pattern of signal intensity change, the lobular structure with high signal intensity on T2-weighted images indicated that the variable proportion of the tumor showed uniform-sized small lobular structures with homogeneous high signal intensity on images of T2-weighted pulse sequences with or without fat-saturation. Full tumor extension included the presence of extraosseous extension with soft tissue mass, epiphyseal involvement in tubular bone, articular involvement, neurovascular invasion, and distant metastasis at initial presentation.

The enhancement pattern was evaluated in post-intravenous gadolinium fat-saturated T1-weighted images. Peripheral rim and septal enhancement pattern indicated a well-enhanced tumor margin and an internal septum of uniformly thin thickness in variable proportion to the tumor. Inhomogeneous enhancement pattern described a global inhomogeneous enhancement in the tumor. Finally, marginal enhancement pattern indicated enhancement in the tumor margin of variable thickness and lack of the lobular structure in the peripheral rim and septal enhancement pattern.

The Mann-Whitney rank test for patient age and mean tumor size, and Fisher's exact test were used for statistical evaluation. Statistical analyses were performed using SPSS version 15.0 (SPSS Inc., Chicago, IL, USA), and p value < 0.05 were considered statistically significant.

Results

Patient ages were statistically different ($p = 0.001$) between chondroblastic OGS and CSA patients, ranging from 10 to 55 years (mean, 24.7 years) in chondroblastic OGS patients and from 23 to 83 years (mean, 56.7 years) in CSA patients. The male-to-female ratio

Table 1. Tumor location

	Chondroblastic OGS ($n=10$)	Chondrosarcoma ($n=10$)	p
Tumor location in the skeleton			
Appendicular:axial bone	8:2	3:7	0.070
Around the knee	7	0	0.003
Tumor distribution within a single bone	($n=8$)	($n=3$)	
Transverse plane (central:peripheral)	5:5	8:2	0.350
Longitudinal plane in appendicular bone (metaphysis:diaphysis:epiphysis)	6:2:0	1:1:1	0.039

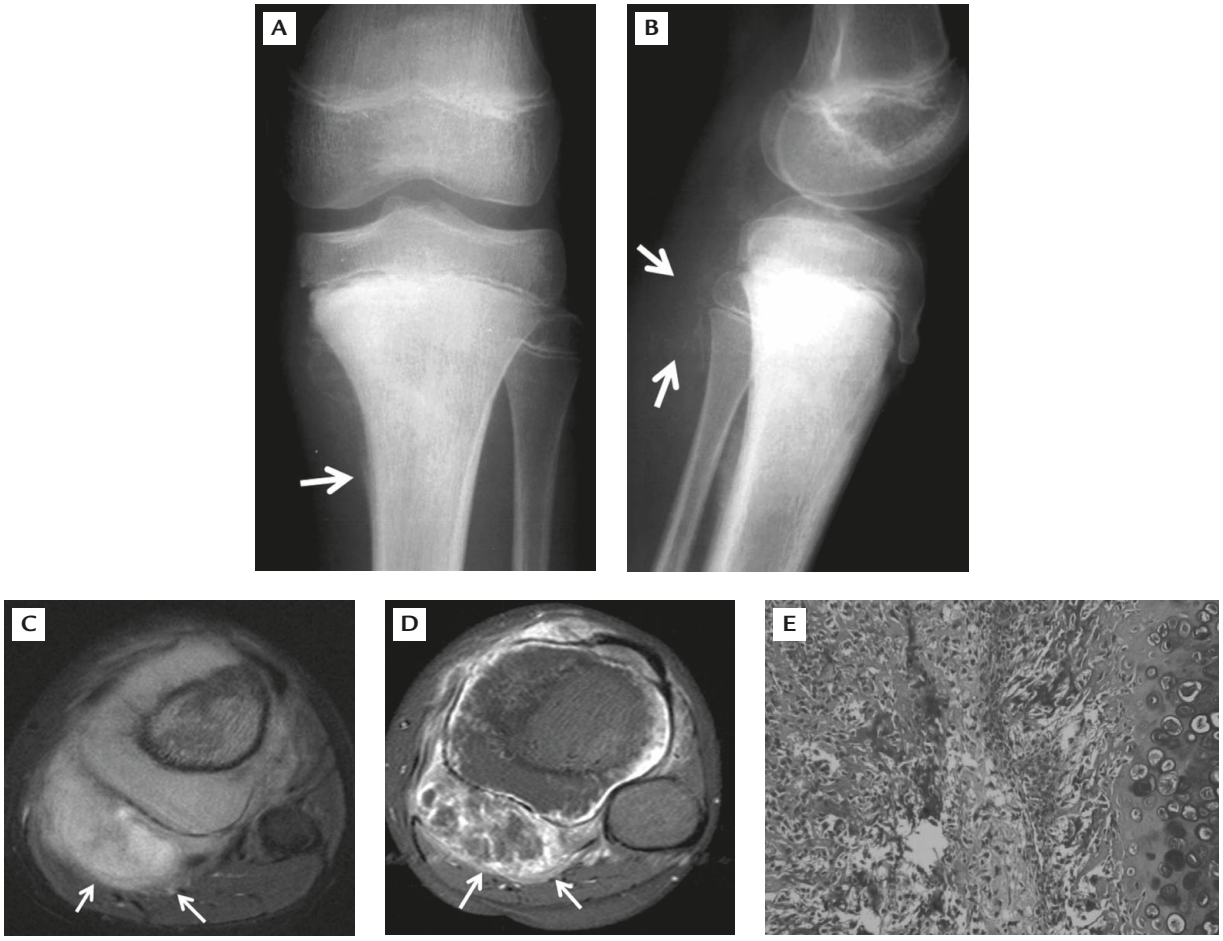

Figure 1. An 18-year-old female patient with chondroblastic osteosarcoma in the left proximal tibia. (A) Anteroposterior radiography of the left knee shows aggressive periosteal reaction, mainly laminated, and Codman's triangle patterns. (B) Lateral radiography shows visible tumor matrix, more in favor of the cartilage-forming pattern. (C) Axial magnetic resonance imaging on fat-saturated T2-weighted imaging shows a lobular structure with high signal intensity. (D) Axial post-intravenous gadolinium fat-saturated T1-weighted imaging shows peripheral rim and septal enhancement in the tumor. (E) Photomicrograph of the histological specimen shows sarcomatous tumor cells that produced both osteoid and chondroid tumor matrices (hematoxylin & eosin; original magnification, 100×).

was 1.5 in chondroblastic OGS and 1 in CSA (p= 1.000). Tumor sizes ranged from 4.3 to 16.4 cm (mean, 8.5 cm) in chondroblastic OGS patients, and from 3.3 to 17.0 cm (mean, 8.5 cm) in CSA patients (p=0.611).

Tumors occurred around the knee in 7 chondroblastic OGS patients and in no CSA patients (p=0.003; Table 1). For tumors in the appendicular bone, tumors originated from the metaphysis in 6 chondroblastic

Table 2. Radiograph analysis of tumor morphology

	Chondroblastic OGS ($n=10$)	Chondrosarcoma ($n=10$)	p
Bone destruction pattern (geographic:moth-eaten:permeative)	0:7:3	0:10:0	0.211
Tumor matrix pattern (absence:bone-forming: cartilage-forming:both:atypical)	0:8:0:2:0	1:0:7:0:2	<0.001
Presence of endosteal scalloping	1	1	1.000
Presence of cortical expansion	3	3	1.000
Presence of cortical penetration	10	9	1.000
Presence of pathologic fracture	1	2	1.000
Periosteal reaction pattern (absence:aggressive:non-aggressive)	3:7:0	9:0:1	0.008

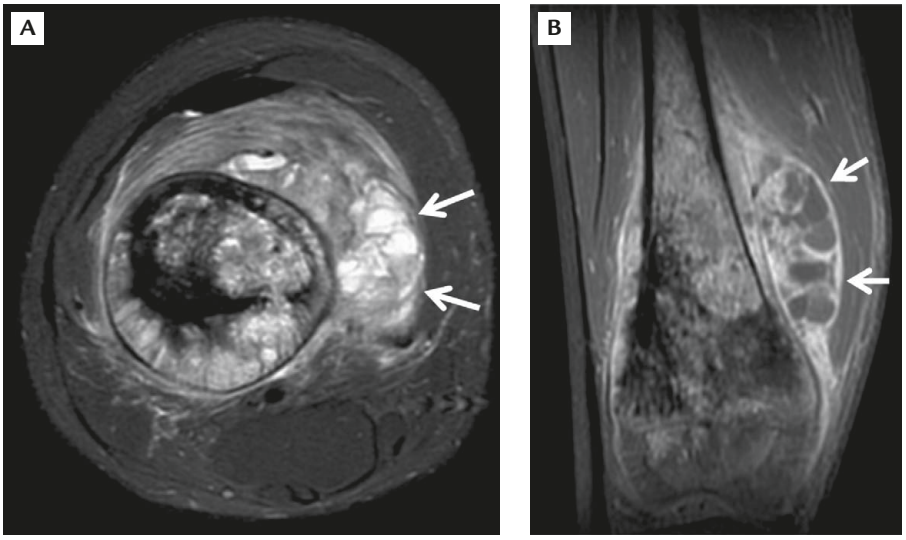

Figure 2. An 11-year-old female patient with chondroblastic osteosarcoma in the right distal femur. (A) Axial magnetic resonance imaging on fat-saturated T2-weighted imaging shows a lobular structure with high signal intensity. (B) Coronal post-intravenous gadolinium fat-saturated T1-weighted imaging shows peripheral rim and septal enhancement in part of the tumor.

OGS and 1 CSA patients and from the diaphysis in 2 chondroblastic OGS and 1 CSA patients. One CSA patient had a tumor that arose in the epiphysis ($p=0.039$). Tumor location around the knee and tumor distribution in the longitudinal plane in the appendicular bone were statistically significantly different between CSA and chondroblastic OGS patients (Table 1).

Visible tumor matrix was present in all 10 patients with chondroblastic OGS, including 8 tumors with the bone-forming pattern and 2 tumors that had both bone- and cartilage-forming patterns (Figure 1B). Nine CSA tumors contained a visible tumor matrix, including cartilage-forming pattern in 7 tumors and atypical radiodensity in 2 tumors. Both the presence and nature of a visible tumor matrix were statistically significantly different between chondroblastic OGS and CSA patients ($p<0.001$; Table 2).

Aggressive periosteal reaction (Figure 1A) was present in 7 chondroblastic OGS, and the main pattern was sunburst in 5 tumors followed by onion-peel in 1 tumor and Codman's triangle in 1 tumor. The presence of aggressive periosteal reaction was statistically significantly different between chondroblastic OGS and CSA patients ($p=0.008$; Table 2). Non-aggressive periosteal reaction was present in 1 CSA, which consisted of a single layer of periosteal reaction. Other tumor morphologies assessed in this study were not statistically significantly different between chondroblastic OGS and CSA (Table 2).

Lobular structures with high signal intensity on T2-weighted images, associated with peripheral rim and septal enhancement pattern, were noted in 2 chondroblastic OGS (Figures 1C, 1D, 2A, 2B and 3) and 10 CSA patients (Figures 4B and 4C) ($p=0.001$). Inhomogeneous and marginal enhancement patterns were noted in 6 and 2 chondroblastic OGS and in no CSA patients, respectively. Finally, full tumor extension as evaluated by MRI was not significantly

different between chondroblastic OGS and CSA patients (Table 3).

Discussion

Conventional OGS most frequently (70–80% of cases) affects tubular bones in the appendicular skeleton, particularly osseous structures around the knee (50–75% of cases).[1–3] CSA occurs in the tubular bones in approximately 45% of cases, and in innominate bone in approximately 25% of cases.[1,2,5] Of the tubular bones, the majority of conventional OGS (80–95%) and approximately half of CSA (49%) arises in the metaphysis, and initial manifestation within the epiphysis is rare in OGS (< 1%) and unusual in CSA (16%).[2,3,5] Although tumor distribution within the transverse plane is seldom discussed in the literature, in this study, tumors occurred more frequently in the central position in CSA and were equally distributed in chondroblastic OGS, though not statistically significant. In this study, only a few cases of CSA occurred in tubular bone and may be due to limited case number. Finally, this study showed that tumor location in the skeleton, around the knee, and in the longitudinal plane in appendicular bone was helpful in the differential diagnosis of chondroblastic OGS and CSA.

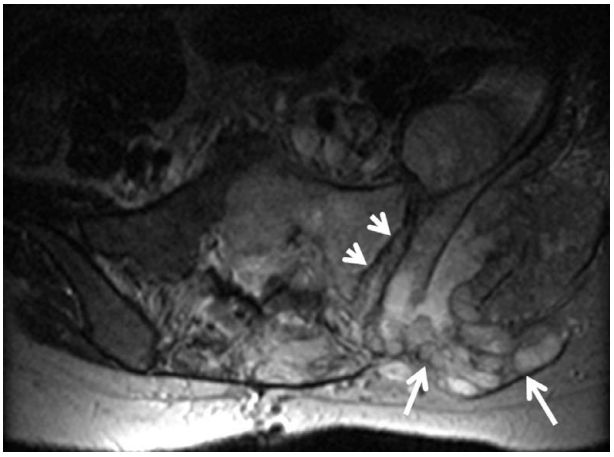

Figure 3. A 23-year-old female patient with chondroblastic osteosarcoma in the left iliac bone. Fat-saturated T2-weighted magnetic resonance imaging reveals a large tumor with a lobular structure and high signal intensity (arrows) as well as tumor invasion of the sacroiliac joint (arrowheads).

Upon radiographic examination, the vast majority (approximately 90%) of OGS demonstrated a variable amount of fluffy and cloudy opacities, characteristic of bone production. Most (approximately 60–79%) CSA demonstrated a variable amount of stippled and fleck-like calcification, characteristic of cartilage production. Conventional tomography (CT) may be required for the detection of cartilage-forming tumor matrix.[1–3,5] This study also revealed that chondroblastic OGS typically possess tumor matrices characteristic of bone-forming, and some possibly also contained a cartilage-forming matrix. The coexistence of these 2 tumor matrices indicates the presence of chondroblastic OGS. Thus, the presence and pattern of visible tumor matrix may provide a useful clue for the differential diagnosis of chondroblastic OGS and CSA.

The host response to aggressive periosteal reaction occurs in 80–90% of OGS, and may be seen in CSA.[1–3,5] Although frequently mixed, the periosteal reaction contained a primarily sunburst appearance, followed by onion-peel and Codman's triangle patterns in OGS.[1–3,5] This study, along with those previously published indicates that the presence of aggressive periosteal reaction is suggestive of OGS, including the chondroblastic subtype.[1–3,5]

The radiographic pattern of bone destruction is indicative of the aggressiveness of the lesion. The geographic

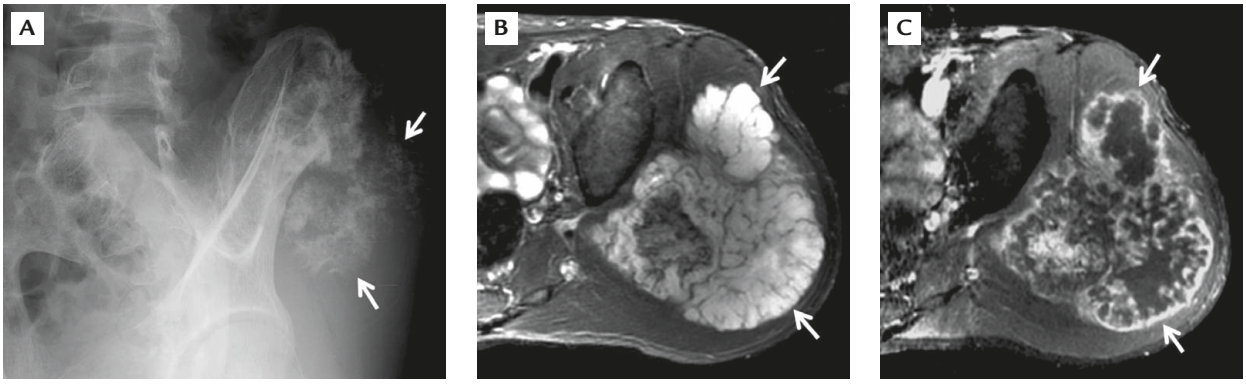

Figure 4. A 23-year-old male patient with chondrosarcoma in the left iliac wing. (A) Oblique pelvic radiography reveals a cartilage-forming tumor matrix. (B) Axial fat-saturated T2-weighted magnetic resonance imaging shows a large tumor with a lobular structure and high signal intensity. (C) Axial post-intravenous gadolinium fat-saturated T1-weighted imaging shows peripheral rim and septal enhancement of the tumor.

Table 3. Magnetic resonance imaging detection of signal intensity changes, enhancement pattern, and tumor extension

	Chondroblastic OGS ($n=10$)	Chondrosarcoma ($n=10$)	p
Lobular high signal intensity on T2-weighted images	2	10	0.001
Enhancement pattern (peripheral rim and septal:inhomogeneous:marginal)	2:6:2	10:0:0	0.001
Tumor extension			
Presence of soft tissue mass	10	9	1.000
Presence of epiphysis involvement in tubular bone	4 ($n=8$)	2 ($n=3$)	0.098
Presence of articular involvement	3	5	0.650
Presence of neurovascular invasion	2	2	1.000
Metastasis at initial presentation	2	1	1.000

pattern was the least aggressive, while the permeative pattern was the most aggressive. Both chondroblastic OGS and CSA showed a more aggressive bone destruction pattern in our study, which was not helpful in their differential diagnosis.

In conventional OGS, inhomogeneous enhancement of the tumor is usually evident.[2,3] Marginal enhancement is often associated with central necrosis of the tumor. The lobular structure with high signal intensity on T2-weighted images, the peripheral rim and septal enhancement pattern, imaging features typical in all hyaline cartilage neoplasm, are seen in 78% of long bone CSA,[5] and might be seen focally or diffusely in some chondroblastic OGS in this study. Geirnaerdt et al reported a much higher incidence of septonodular enhancement in 78% (7/9) and peripheral rim and septal enhancement pattern in 22% (2/9) of chondroblastic OGS, probably because they compared MRI findings with histopathologic findings, and even the presence of these enhancement patterns in only a minority of tumors would be recorded.[10]

MRI is crucial in the evaluation of intra- and extraosseous extension of a tumor. Of particular importance for the therapy plan (limb-sparing procedure) is the relationship between the soft tissue extension and the neurovascular bundles.[1–4] However, this study showed that tumor extension in MRI was not useful for the differential diagnosis of chondroblastic OGS and CSA.

Most of the patients with conventional OGS were in their 2nd and 3rd decades of life, and some were ≥50 years of age.[1–3] However, the majority of patients with CSA were ≥50 years old.[1,2,5] Because the chondroblastic OGS patients were much younger than the CSA patients, age may be helpful in their differential diagnosis.

The absence of histopathologic correlation with the imaging features suggestive of abundant hyaline cartilage in chondroblastic OGS represents a limitation of this study. The categorization of tumor matrix into bone- or cartilage-forming was equivocal when the tumor matrix was small and faint, and the presence of peripheral rim and septal enhancement pattern was equivocal when present in only a minority of the tumor. Thus, the pattern of periosteal reaction of chondroblastic OGS was frequently mixed, and choosing the major pattern subjectively may be inadequate.

In conclusion, the presence of a visible bone-forming tumor matrix as well as aggressive periosteal reaction, younger patient age, and tumor occurrence in the metaphysis of the appendicular bone and around the knee were more in favor of chondroblastic OGS. Some chondroblastic OGS showed imaging features reflecting pathohistologically abundant hyaline cartilage components, including the coexistence of bone- and cartilage-forming tumor matrix on radiographs, presence of lobular structure of high signal intensity on T2-weighted images, and peripheral rim and septal enhancement pattern on MRI. Avoiding tumor areas with those imaging features in chondroblastic OGS might improve the biopsy accuracy.

References

1. Dorfman HD, Czerniak B. *Bone Tumors*. St Louis: Mosby, 1997.
2. Resnick D, Kransdorf MJ. *Bone and Joint Imaging*, 3rd edition. Philadelphia: Elsevier Saunders, 2005.
3. Murphey MD, Robbin MR, McRae GA, Flemming DJ, Temple HT, Kransdorf MJ. The many faces of osteosarcoma. *Radiographics* 1997;17:1205–31.
4. Huang TL, Chen TH, Chen Winby YK, Chen WM, Liu CL, Lo WH. Allograft arthrodesis of the knee in high-grade osteosarcoma. *J Chin Med Assoc* 2005;68:425–30.
5. Murphey MD, Walker EA, Wilson AJ, Kransdorf MJ, Temple HT, Gannon FH. From the archives of the AFIP: imaging of primary chondrosarcoma: radiologic-pathologic correlation. *Radiographics* 2003;23:1245–78.

6. Bacci G, Bertoni F, Longhi A, Ferrari S, Forni C, Biagini R, Bacchini P, et al. Neoadjuvant chemotherapy for high-grade central osteosarcoma of the extremity. *Cancer* 2003;97: 3068–75.
7. Hauben EI, Weeden S, Pringle J, Van Marck EA, Hogendoorn PCW. Does the histological subtype of high-grade central osteosarcoma influence the response to treatment with chemotherapy and does it affect overall survival? A study on 570 patients of two consecutive trials of the European Osteosarcoma Intergroup. *Eur J Cancer* 2002;38:1218–25.
8. Ilaslan H, Sundaram M, Unni KK, Shives TC. Primary vertebral osteosarcoma: imaging findings. *Radiology* 2004;230: 697–702.
9. Lee YY, Van TP, Nauert C, Raymond AK, Edeiken J. Craniofacial osteosarcomas: plain film, CT, and MR findings in 46 cases. *AJR Am J Roentgenol* 1988;150:1397–402.
10. Geirnaerdt MJ, Bloem JL, van der Woude HJ, Taminiau AH, Nooy MA, Hogendoorn PC. Chondroblastic osteosarcoma: characterization by gadolinium-enhanced MR imaging correlated with histopathology. *Skeletal Radiol* 1998;27:145–53.